

10 Gb/s two-dimensional free-space optical code division multiple access wiretap channel with spatial diversity

Jianhua Ji (吉建华)*, Jianjia Zhang (张建佳), Bing Wu (巫兵), Ke Wang (王可),
and Ming Xu (徐铭)

Shenzhen Key Laboratory of Communication and Information Processing, College of Information Engineering,
Shenzhen University, Shenzhen 518060, China

*Corresponding author: jjh@szu.edu.cn

Received March 19, 2019; accepted May 13, 2019; posted online July 15, 2019

We experimentally demonstrate a 10 Gb/s free-space optical wiretap channel based on a spatial-diversity scheme and optical code division multiple access. In weak and middle turbulence cases, the bit error rate of a legitimate user can be decreased, and physical layer security can be simultaneously enhanced.

OCIS codes: 060.2605, 060.4785.

doi: 10.3788/COL201917.080604.

Over the past few years, free-space optical (FSO) communication has attracted considerable attention for a variety of applications^[1,2]. However, FSO communications are highly susceptible to atmospheric turbulence, as a result of the variations in the refractive index due to inhomogeneities in temperature and pressure changes. Many methods have been proposed to overcome the effects of turbulence-induced fading. Diversity is an effective method to improve the data rate and the reliability of communications over fading channels^[3]. Diversity techniques used in wireless communication include time diversity, frequency diversity, and spatial diversity.

On the other hand, FSO communications can still suffer from optical tapping risks^[4,5]. Optical code division multiple access (OCDMA) can improve the physical-layer security of optical communication systems^[6-9]. To enhance the reliability and security in FSO systems, in this Letter we propose and demonstrate a 10 Gb/s FSO wiretap channel based on spatial diversity and an OCDMA scheme. A 10 Gb/s two-dimensional (2D) optical encoder and decoder are constructed based on wavelength selective switch (WSS) DROP/ADD devices and optical delay lines (ODLs). Experiments show that reliability and security can be simultaneously enhanced.

Figure 1 shows a 2D FSO-CDMA wiretap channel with spatial diversity. The 10G transmitter outputs optical pulses with a width of 15 ps and a spectrum of 1548.7–1550.1 nm, corresponding to the WSS wavelengths of 53 (1549.72 nm), 54 (1550.12 nm), and 55 (1550.52 nm). The output power is -3.48 dBm. After erbium-doped fiber amplifier (EDFA) amplification, a 2D optical encoder is used for optical coding. We use modified prime frequency hopping codes [(13,53), (52,54), (65,55)], where (i, j) denotes the position of the i th chip pulse and the j th wavelength^[10].

The encoded optical signal is amplified by EDFA and transmitted to an optical coupler. Each output port is

connected with an ODL to adjust the relative delays. Then, each optical-coded signal is emitted to an atmosphere channel through a collimator lens. The two collimator lenses are 12 cm apart. The transmission distance is 1.8 m. In order to simulate the atmospheric turbulence effect, a 40 cm \times 40 cm \times 80 cm carton is designed. The small holes at the left and right ends are used for optical signal transmission. The hot air is provided by the electric hair dryer. Different temperatures and wind speeds correspond to different turbulence effects.

At the receiving end, each collimator lens receives the optical signals, respectively, which are combined by an optical coupler. A tunable attenuator is used to simulate different receiving powers. Then, a matched 2D optical decoder is used for optical decoding. After EDFA amplification, photoelectric detection (PD) is carried out, and the 10G bit error rate (BER) tester is used for error detection. At the same time, an eavesdropper (Eve) intends to obtain useful information with an extraction ratio. Since the laser beam experiences divergence due to optical diffractions, one possibility for a successful eavesdropping is to locate Eve in the divergence region of the beam. It is reasonably easy for the legitimate user to change the optical code. Hence, we assume that the optical code of the legitimate user should not be available for Eve. The waveform and eye diagram are tested by a 20G DPO72004 C digital phosphor oscilloscope.

As shown in Fig. 2, since the WSS has eight input and output ports, we can use prime frequency hopping codes^[10]. For example, [(0,0), (13,1), (26,2), (39,3), (52,4), (65,5), (78,6), (91,7)] with code length 169 and code weight 8. In this experimental system, the 10G optical transmitter outputs three wavelengths corresponding to WSS (53, 54, 55). Hence, three ports (2, 5, 6) of WSS DROP and WSS ADD are used to encode and decode optical signals, and the corresponding address code is [(13,53), (52,54), (65,55)]. For WSS encoder, delays of ODL2,

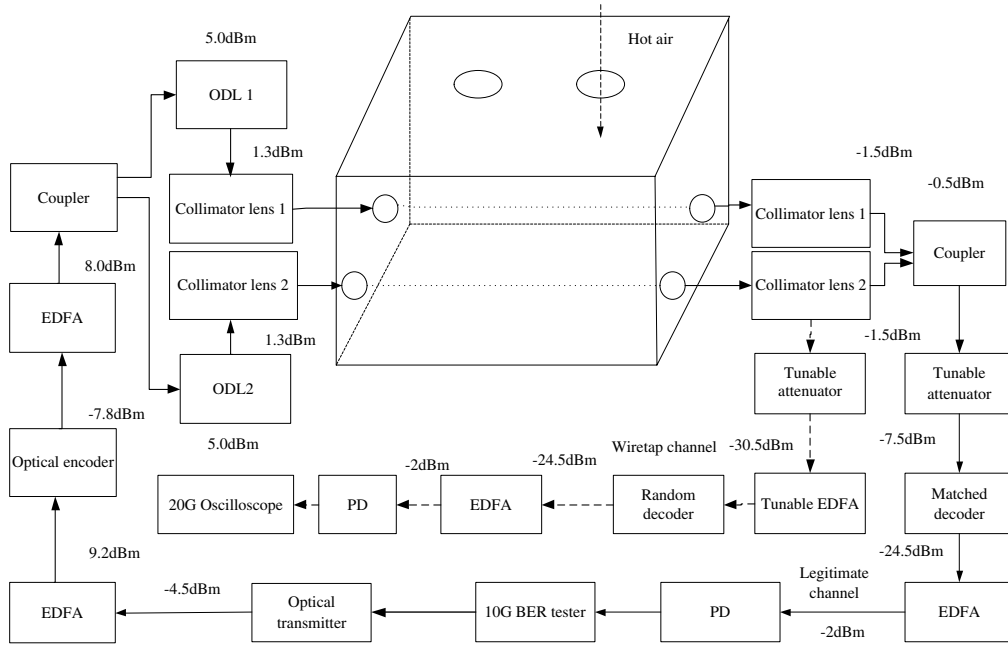


Fig. 1. 10 Gb/s 2D FSO-CDMA wiretap channel.

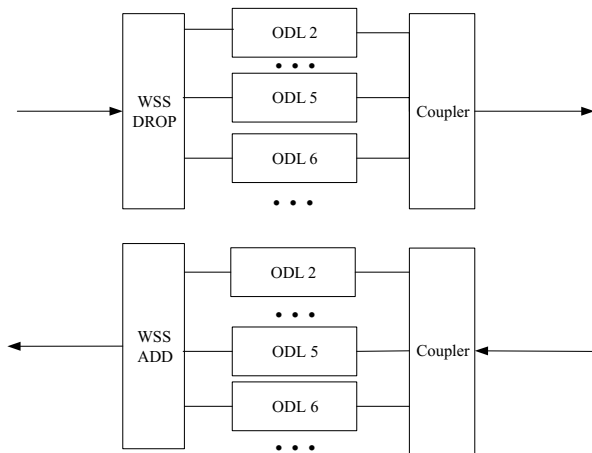


Fig. 2. Optical encoder and decoder based on WSS and ODLs.

ODL5 and ODL6 are 7.1 ps, 30.2 ps, and 37.9 ps, respectively. For the WSS decoder, delays of ODL2, ODL5, and ODL6 are 92.9 ps, 69.8 ps, and 62.1 ps, respectively.

Different turbulence conditions can be simulated by controlling different hot wind temperatures and wind speeds. Figure 3 shows the received signal waveforms for two different turbulence cases. The x label indicates the sampling time, and the y label indicates the signal amplitude. The test time is 10 s and the sampling interval is 0.01 ms. The variance can be calculated by

$$\sigma_I^2 = \langle I_1^2 \rangle / \langle I_1 \rangle^2 - 1,$$

where I_1 is the received intensity after passing through the turbulent channel. Then we can obtain the refractive index structure coefficient

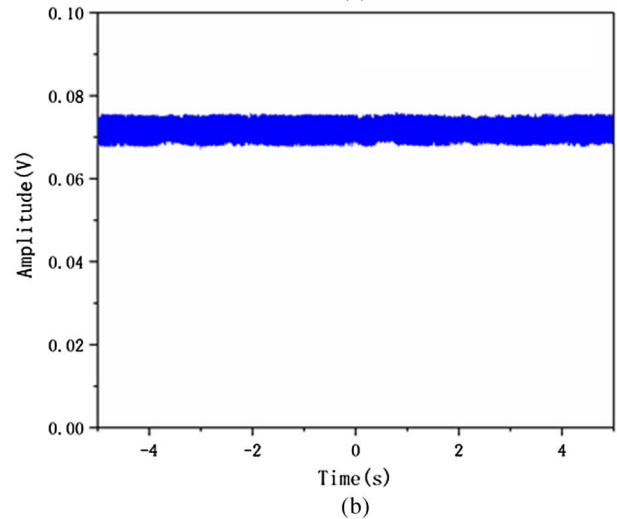
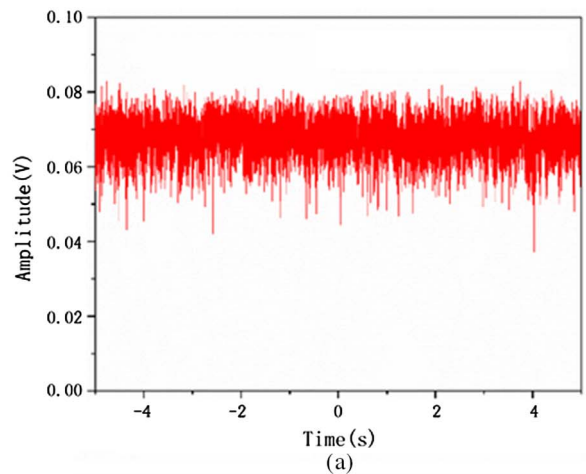


Fig. 3. Received signal waveforms: (a) middle turbulence and (b) weak turbulence.

$$C_n^2 = \frac{\sigma_I^2}{1.23} k^{-7/6} L^{-11/6},$$

where k is wave number and L is the link distance in meters^[1]. The obtained normalized variance of middle atmospheric turbulence is 0.017 and C_n^2 is 3.41×10^{-14} ; and for weak turbulence the normalized variance is 0.003 and C_n^2 is 4.96×10^{-15} .

Figure 4 shows the eye diagrams of weak and middle turbulence conditions at a received power -9.3 dBm. The x label of the eye diagram in Fig. 4 represents the sampling time, 40 ps/div; and the y label represents the amplitude of the signal, 30 mV/div. Figure 5 shows the BERs in weak and middle turbulence conditions. Here, the x label P_r (dBm) is the received power at the optical decoder, and the y label represents the BER of the legitimate user. Note that, compared with the no diversity scheme, the BER performance of two-spatial diversity can be improved by about one order of magnitude. For example, when the received power is -7.5 dBm in the middle turbulence, the BER will be 7.4×10^{-8} and 4.8×10^{-7} in the two-spatial diversity and no-diversity FSO-CDMA wiretap channels, respectively.

Figure 6 shows Eve's eye diagrams with encoded and uncoded conditions in weak turbulence, where the received power is -9.3 dBm and an Eve extract of 1% of optical power (corresponding to extract ratio 0.5% in no diversity). Note that Eve will not be able to recover the user's data of the encoded system, while Eve can recover the data in the uncoded system.

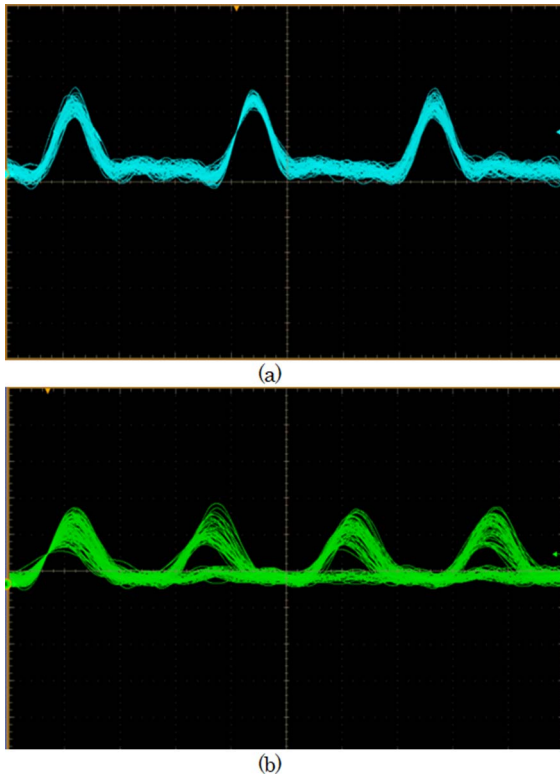


Fig. 4. Eye diagrams of middle turbulence: (a) diversity and (b) no diversity.

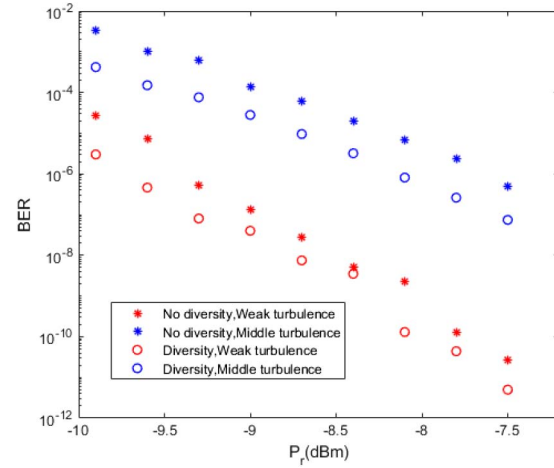


Fig. 5. BERs in weak and middle turbulence conditions.

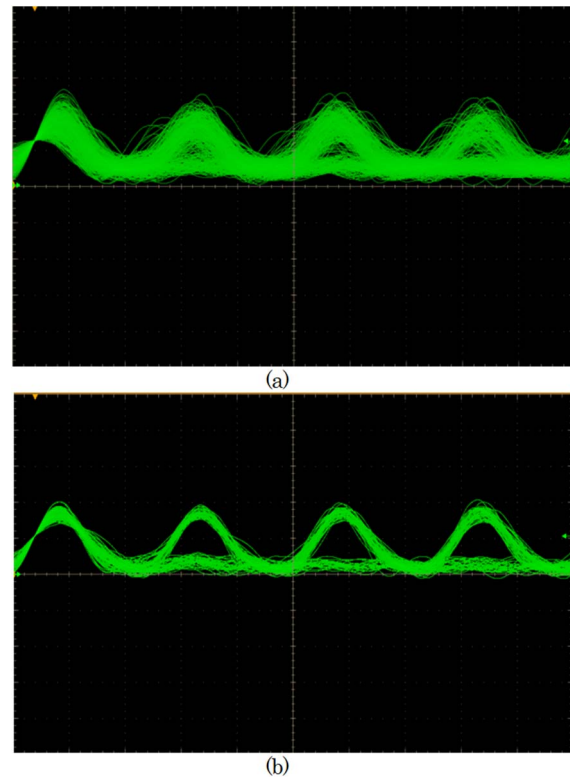


Fig. 6. Eve's eye diagrams with an extract ratio of 1%: (a) encoded and (b) uncoded.

Figure 7 shows Eve's BER with an extract ratio of 1%. Here, EDFA is used by Eve, and the optical power at PD is -2 dBm. In Fig. 7, the x label P_r (dBm) represents the received power at the optical decoder, and the y label represents the BER of the eavesdropper. The BER of the eavesdropper will decrease with the increase of the received power. Note that Eve's BER will deteriorate seriously under encoded circumstances, which demonstrates the enhancement of physical-layer security in spatial-diversity FSO-CDMA systems. For example, when the received power is -9.0 dBm in weak turbulence,

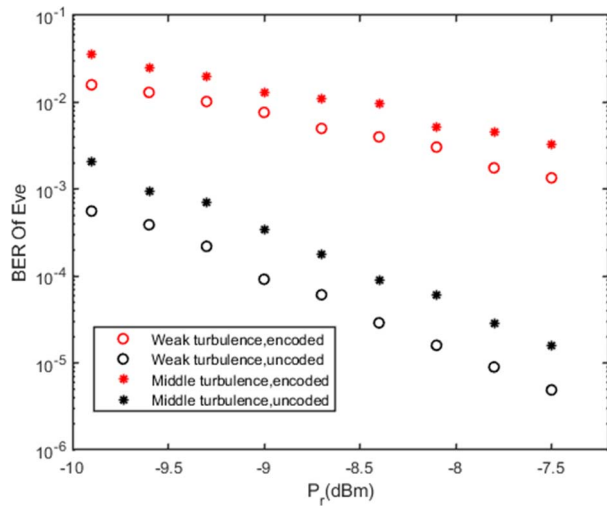


Fig. 7. Eve's BER with an extract ratio of 1%.

the BER will be 1.02×10^{-2} and 2.2×10^{-4} in encoded and uncoded FSO-CDMA wiretap channels, respectively.

Compared with the no-diversity FSO system, the spatial-diversity FSO system can improve the reliability of the system. However, for the uncoded FSO system, spatial diversity cannot improve the physical layer security. Therefore, the spatial-diversity FSO system has security risks.

In this Letter, we propose and demonstrate 10 Gb/s 2D FSO-CDMA wiretap channels with spatial diversity. By employing spatial diversity and an OCDMA scheme, reliability and security can be simultaneously enhanced in an FSO system. However, compared with uncoded

FSO systems, the disadvantage of this scheme is that the complexity is increased.

It should be pointed out that, when the frequency of codeword reconstruction is high enough, Eve will not be able to track the changes of the codeword of the legitimate user.

This work was supported by the National Natural Science Foundation of China (NSFC) (No. 61671306) and the Fundamental Research Project of Shenzhen (JCYJ) (No. 20160328145357990).

References

1. J. Hu, Z. Zhang, L. Wu, J. Dang, and G. Zhu, *Chin. Opt. Lett.* **16**, 120101 (2018).
2. J. Yin, H. Liu, R. Huang, Z. Gao, and Z. Wei, *Chin. Opt. Lett.* **15**, 060101 (2017).
3. M. A. Khalighi and M. Uysal, *IEEE Commun. Surv. Tutorials* **16**, 2231 (2014).
4. F. J. Lopez-Martinez, G. Gomez, and J. M. Garrido-Balsells, *IEEE Photonics J.* **7**, 7901014 (2015).
5. H. Endo, T. S. Han, T. Aoki, and M. Sasaki, *IEEE Photonics J.* **7**, 7903418 (2015).
6. Z. Wang, J. Chang, and P. R. Prucnal, *J. Lightwave Technol.* **28**, 1761 (2010).
7. J. Ji, G. Zhang, W. Li, L. Sun, K. Wang, and M. Xu, *J. Opt. Commun. Netw.* **9**, 813 (2017).
8. L. Tancevski, I. Andonovic, M. Tur, and J. Budin, *IEEE Photonics Technol. Lett.* **8**, 935 (1996).
9. J. Ji, X. Chen, and Q. Huang, *IET Commun.* **13**, 116 (2019).
10. L. Tancevski and I. Andonovic, *Electron. Lett.* **30**, 1388 (1994).
11. L. A. Rusch, M. Abtahi, P. Lemieux, W. Mathlouthi, and L. A. Rusch, *J. Lightwave Technol.* **24**, 4966 (2007).